Arctic Polar Vortex Controls Aerosol Evolution After High-Latitude Volcanic Eruptions

Herman F. Fuglestvedt[1], Zhihong Zhuo[1], Matthew Toohey[2], and Kirstin Krüger[1]

[1]Department of Geosciences, University of Oslo, Oslo, Norway

[2]Institute of Space and Atmospheric Studies, University of Saskatchewan, Saskatoon, SK, Canada

UNIVERSITY OF OSLO

Motivation and Questions

High-latitude explosive eruptions inject gases and material into the polar stratosphere. Since the strength, location, and stability of the Arctic polar vortex is highly variable, we ask:

- ▶ **How does the Arctic polar vortex state influence volcanic aerosol evolution?**
- ▶ **Is it relevant for the volcanic forcing?**
- ▶ **Which properties of the polar vortex matter?**

Summary and Conclusions

- ▶ **The Arctic polar vortex controls the radiative forcing from high-latitude winter SO_2 injections.** Initial polar vortex state determines the equatorward SO_2 transport (Fig. 1), significantly impacting stratospheric aerosol optical depth (SAOD) (Fig. 3d).
- ▶ **Enhanced equatorward transport reduces SO_2 e-folding time** as the low-latitude OH abundance expedites oxidation (Fig. 2b).
- ▶ **Enhanced equatorward transport reduces aerosol growth, amplifying radiative forcing.** Cumulative and peak SAOD vary up to 27 % and 12 %, respectively (Fig. 3d), depending on the meridional dispersal of the SO_2 from the first month after eruption.
- ▶ **The polar vortex's stability in the first few weeks controls SO_2 transport.** Neither zonal wind nor temperature alone correlate with the SO_2 e-folding time.

Model and Experiments

- ▶ High-top aerosol-chemistry Earth system model **CESM2-WACCM6*** [1–3]
- ▶ **Icelandic explosive eruptions**† of Pinatubo-magnitude
- ▶ **Sulphur, chlorine, and bromine** co-injection‡
- ▶ **Six polar vortex initial conditions** (Fig. 2)

*1850 background conditions, 1°-resolution.
†64°N, 19°W (Katla volcano) [4, 5]. 24 km altitude on January 1.
‡17 Tg SO_2, 2.93 Tg HCl, and 9.5 Gg HBr. Halogen loads based on average Central American Volcanic Arc emissions [6, 7], assuming 10 % injection efficiency [8–11].

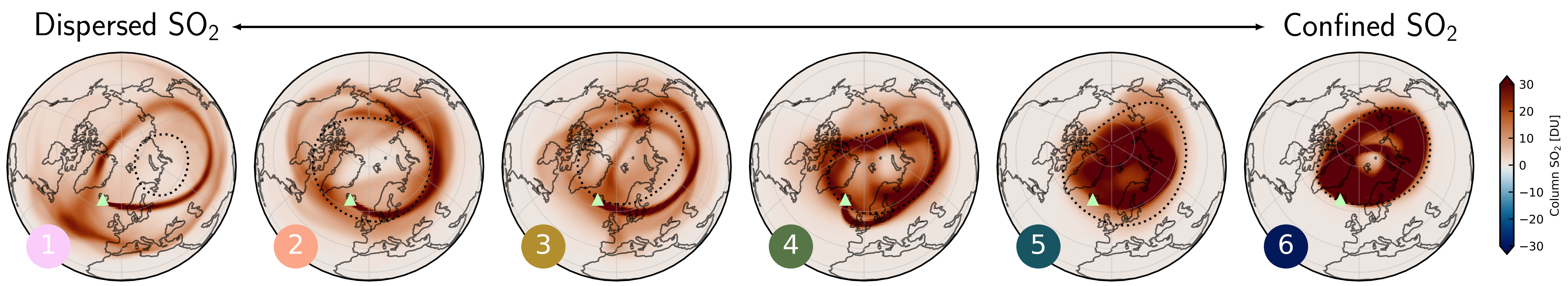

Fig. 1: **The polar vortex state controls the initial transport of SO_2.** In ensemble members 1-6, the volcanic SO_2 is either transported towards the equator or confined to the polar latitudes, depending on the initial condition of the polar vortex (see Fig. 2). The plot shows the mean column SO_2 in the first month following the eruption (January) as well as the monthly mean 24 km geopotential height contour (dotted).

Sensitivity Experiments

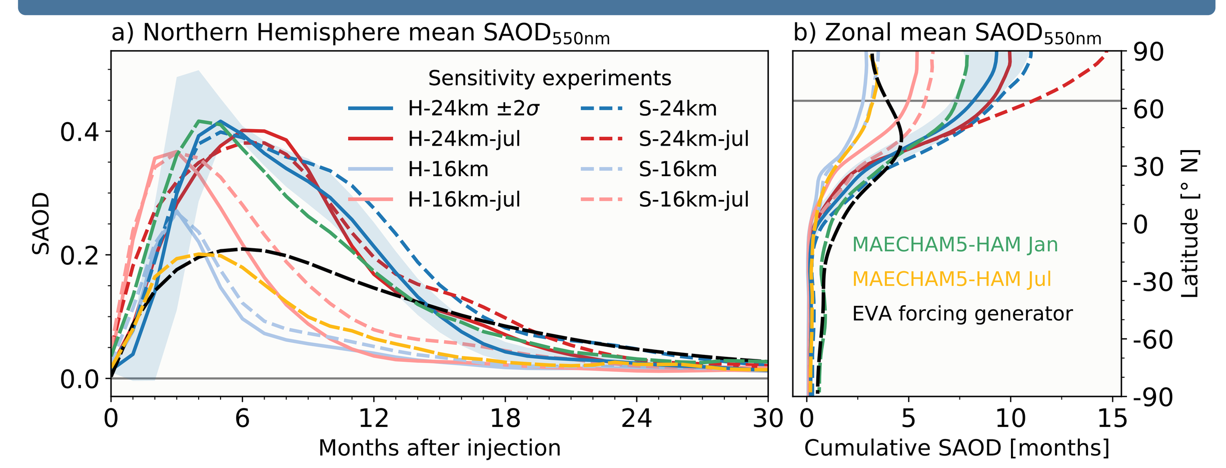

Fig. 4: **The sensitivity of volcanic forcing to the initial polar vortex state is comparable to the sensitivity to several eruption source parameters and inter-model disagreement.** a) Time evolution and b) meridional profile of stratospheric aerosol optical depth for the baseline scenario ensemble with varying initial polar vortex states (labelled H-24km), as well as sensitivity experiments (where H denotes sulphur+halogens and S denotes sulphur-only experiments), the aerosol-general circulation model MAECHAM5-HAM [13], and the Easy Volcanic Aerosol forcing generator (EVA) [14].

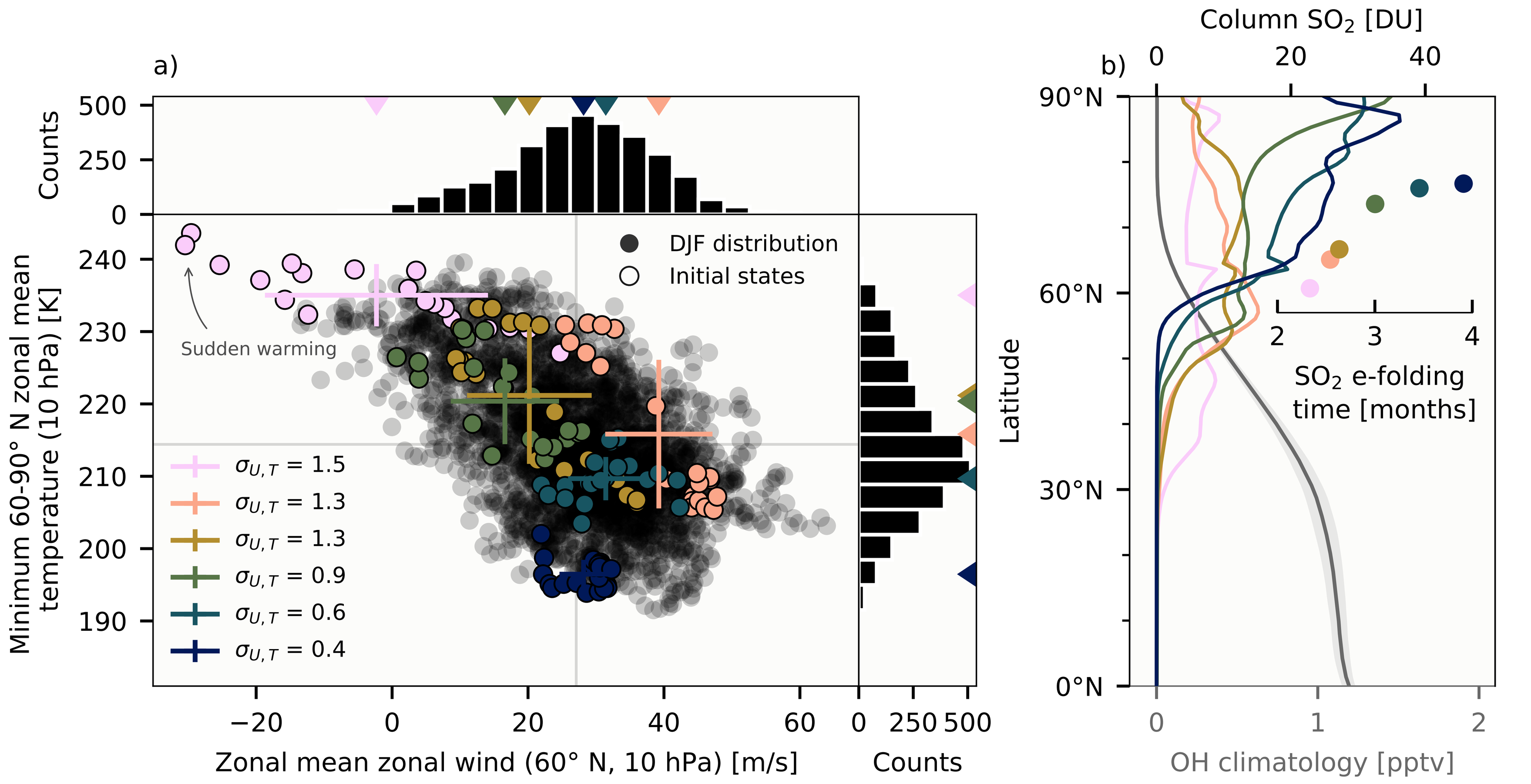

Fig. 2: **The stability of the initial polar vortex determines SO_2 transport and its lifetime**. a) DJF daily mean polar vortex wind and temperature distribution in the control (black circles/histograms/lines) with highlighted January 1-20 of each ensemble member. Errorbars represent 1σ standard deviations centred on means. $\sigma_{U,T}$, the sum of the initial states' wind and temperature standard deviations normalised by corresponding DJF standard deviations, quantifies the two-dimensional spread of each 20-day cluster. b) Meridional profiles of January mean zonal mean column SO_2 (top abscissa) and the January mean zonal mean OH model climatology at 24 km (bottom abscissa). Inset shows the relationship between latitude-centre of mass of SO_2 profiles and SO_2 e-folding time.

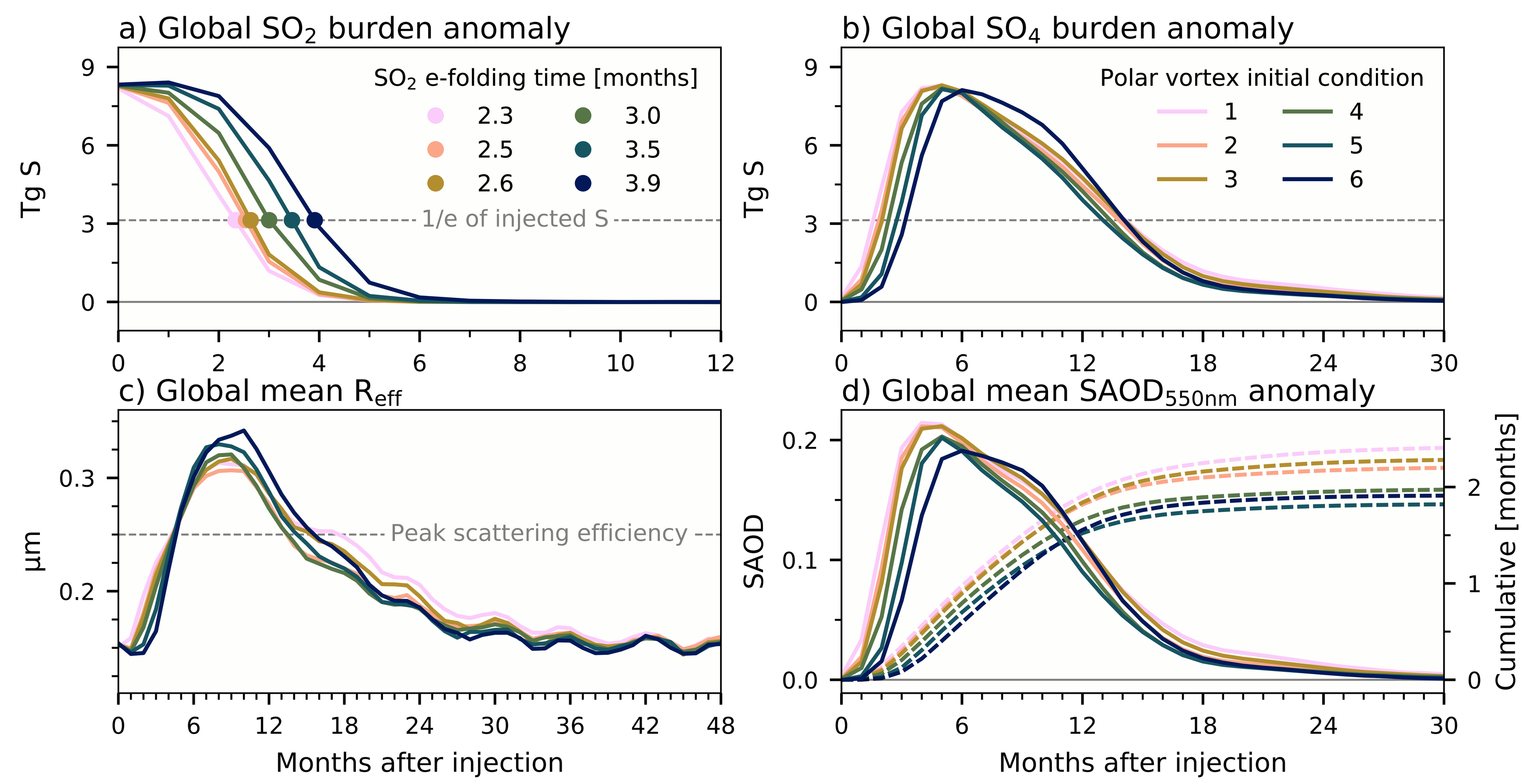

Fig. 3: **Aerosol formation rate, sizes, and radiative forcing.** a) Equatorward transport impacts SO_2 e-folding time (seen in Fig. 1, 2b). b) SO_4 aerosol formation mirrors the SO_2 oxidation rate. c) Aerosol size (R_{eff}) is modulated by aerosol formation and growth, both depending on initial SO_2 transport. Dashed line: The peak scattering efficiency of volcanic SO_4 as a function of R_{eff} [12]. d) Peak stratospheric aerosol optical depth (SAOD) (left ordinate) is increased for the ensemble members with smaller aerosols during peak SO_4 burden. These members also show slightly longer SO_4 lifetimes due to weaker gravitational settling, resulting in generally larger cumulative SAOD (right ordinate). Note the different time axes.

References

1. Danabasoglu, G. *et al.* The Community Earth System Model version 2 (CESM2). *Journal of Advances in Modeling Earth Systems* **12,** e2019MS001916 (2020).
2. Gettelman, A. *et al.* The Whole Atmosphere Community Climate Model Version 6 (WACCM6). *Journal of Geophysical Research: Atmospheres* (2019).
3. Mills, M. J. *et al.* Radiative and chemical response to interactive stratospheric sulfate aerosols in fully coupled CESM1 (WACCM). *Journal of Geophysical Research: Atmospheres* **122,** 13–061 (2017).
4. Óladóttir, B. A., Larsen, G., Thordarson, T. & Sigmarsson, O. The Katla volcano S-Iceland: Holocene tephra stratigraphy and eruption frequency. *Jökull* **55,** 53–74 (2005).
5. Óladóttir, B. A., Sigmarsson, O., Larsen, G. & Thordarson, T. Katla volcano, Iceland: magma composition, dynamics and eruption frequency as recorded by Holocene tephra layers. *Bulletin of Volcanology* **70,** 475–493 (2008).
6. Kutterolf, S. *et al.* Combined bromine and chlorine release from large explosive volcanic eruptions: A threat to stratospheric ozone? *Geology* **41,** 707–710 (2013).
7. Kutterolf, S. *et al.* Bromine and chlorine emissions from Plinian eruptions along the Central American Volcanic Arc: From source to atmosphere. *Earth and Planetary Science Letters* **429,** 234–246 (2015).
8. Brenna, H., Kutterolf, S. & Krüger, K. Global ozone depletion and increase of UV radiation caused by pre-industrial tropical volcanic eruptions. *Scientific reports* **9,** 1–14 (2019).
9. Brenna, H., Kutterolf, S., Mills, M. J. & Krüger, K. The potential impacts of a sulfur-and halogen-rich supereruption such as Los Chocoyos on the atmosphere and climate. *Atmospheric Chemistry and Physics* **20,** 6521–6539 (2020).
10. Rose, W. I. *et al.* Atmospheric chemistry of a 33–34 hour old volcanic cloud from Hekla Volcano (Iceland): Insights from direct sampling and the application of chemical box modeling. *Journal of Geophysical Research: Atmospheres* **111** (2006).
11. Textor, C., Graf, H.-F., Herzog, M. & Oberhuber, J. Injection of gases into the stratosphere by explosive volcanic eruptions. *Journal of Geophysical Research: Atmospheres* **108** (2003).
12. Lacis, A. Volcanic aerosol radiative properties. *Past Global Changes Magazine* **23,** 50–51 (2015).
13. Toohey, M. *et al.* Disproportionately strong climate forcing from extratropical explosive volcanic eruptions. *Nature Geoscience* **12,** 100 (2019).
14. Toohey, M., Stevens, B., Schmidt, H. & Timmreck, C. Easy Volcanic Aerosol (EVA v1. 0): an idealized forcing generator for climate simulations. *Geoscientific Model Development* **9,** 4049–4070 (2016).

EGU General Assembly 23–28 April 2023